Low-Temperature Internal Friction in Face-Centered Cubic and Body-Centered Cubic Metals*†

L. J. BRUNER‡§
Department of Physics and Institute for the Study of Metals, University of Chicago, Chicago, Illinois
(Received November 2, 1959)

Data on the anelasticity produced by plastic deformation in various face-centered cubic and body-centered cubic pure metals and alloys are reported. Fcc materials studied at temperatures from 4.2°K to 300°K include Cu, Al, and Al—0.25 at. % Cu. Bcc systems are Fe, Nb, and β brass. Bordoni peaks are observed in Cu and Al in agreement with previous work, but are not found in either strain aged Al—Cu alloys or pure Fe. A peak observed in Nb at 173°K is not believed to be a Bordoni type. Unexplained low-temperature internal friction peaks are also observed in β brass. A new mechanism is proposed for dislocation relaxation in which the essential feature is the thermally activated motion of paired partial dislocations between vacancy pinning points. It is in general qualitative accord with experiment, and permits semiquantitative evaluation of all essential parameters.

I. INTRODUCTION

THIS investigation of internal friction in fcc and bcc metals and alloys was undertaken with the intention of making a systematic survey of the origin and character of the low-temperature internal friction peaks exhibited by some plastically deformed metals. These peaks, originally observed by Bordoni[1] in the four fcc metals Cu, Ag, Al, and Pb, and subsequently studied by various investigators,[2–8] have the following characteristics:

(1) They occur only in plastically deformed metals, being sharply attenuated or completely absent in recrystallized material.

(2) They have their origin in thermally activated processes, exhibiting in a general way the exponential temperature dependence of the relaxation time predicted by the Arrhenius equation. In addition a modulus defect on transition from unrelaxed to relaxed behavior is observed in accordance with the elementary theory of the mechanical relaxation process.[9]

(3) They cannot be described in terms of a single relaxation process; a multiplicity of relaxation times is involved in each case.

The first of these characteristics indicates that the high density of dislocations present in plastically deformed materials is responsible for the peaks. All efforts to develop a satisfactory model for the relaxation process have started from this premise. These will be reviewed briefly during the course of this paper in connection with the presentation of a new mechanism for dislocation relaxation, based upon the thermally activated motion of paired partial dislocations between vacancy pinning points. This model appears to account more satisfactorily for the results of this and preceding investigations than previous theories.

In Sec. II our experimental procedure is outlined. Section III summarizes all data taken. In Sec. IV we discuss the principal experimental evidence provided by this and previous investigations, and show how it leads us to consider the new mechanism mentioned above. The formal development of our model is presented in Sec. V. In Sec. VI we complete the quantitative comparison of our model with experiment, and summarize its advantages as well as the difficulties which remain unresolved.

II. EXPERIMENTAL METHOD

Internal friction is measured by the free decay method in bars 1 cm in diameter and either 10 cm or 20 cm long. They are driven in longitudinal modes of vibration. The specimen holder and its associated apparatus is illustrated in Fig. 1. The sample is supported nodally at its center by needle points. A polarized ac voltage is applied between it and a driving plate placed close to its upper end. This electrostatic drive has the advantage that it avoids the introduction of thermoelastic strains arising from differential thermal expansion between the sample and an attached transducer. Furthermore, extraneous sources of loss are minimized permitting more reliable measurement of loss at very low temperatures.

This assembly is placed in a helium and nitrogen double Dewar of conventional design. Temperature control is facilitated by the use of activated charcoal as

* Submitted as a thesis in partial fulfillment of the requirements for the degree of Doctor of Philosophy at the University of Chicago.

† This work was supported in part by the Office of Naval Research and in part by a grant from the National Science Foundation for low-temperature research, under the direction of Professor E. A. Long.

‡ Now at International Business Machines Watson Laboratory at Columbia University, New York, New York.

§ National Science Foundation Predoctoral Fellow, 1954–57.

[1] P. G. Bordoni, J. Acoust. Soc. Am. **26**, 495 (1954).

[2] D. H. Niblett and J. Wilks, Phil. Mag. **2**, 1427 (1957).

[3] J. S. Hutcheson and G. J. Hutton, Can. J. Phys. **36**, 82 (1958).

[4] H. L. Caswell, J. Appl. Phys. **29**, 1210 (1958).

[5] H. L. Caswell, Cornell thesis, 1957 (unpublished).

[6] V. K. Pare, Cornell thesis, 1958 (unpublished).

[7] D. O. Thompson and D. K. Holmes, J. Appl. Phys. **30**, 525 (1959).

[8] P. G. Bordoni, M. Nuovo, and L. Verdini, Phys. Rev. Letters **2**, 200 (1959).

[9] C. Zener, *Elasticity and Anelasticity of Metals* (University of Chicago Press, Chicago, 1949), p. 41.

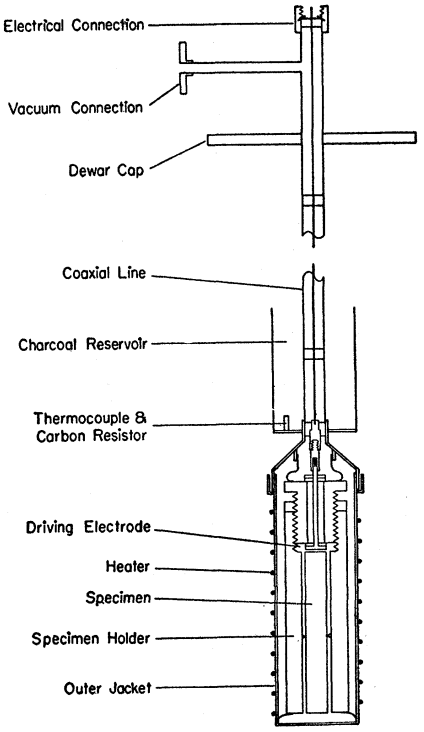

FIG. 1. The specimen holder and associated apparatus.

a thermal ballast, providing base warmup rates of no greater than 2°K per hour. Thermal equilibrium between specimen and measuring elements is insured by all copper construction of the lower assembly, together with the use of helium exchange gas which is pumped out just prior to each measurement. A carbon resistance thermometer covers the temperature range below 20°K, a copper-constantan thermocouple is used at higher temperatures. The calibration of these elements is established by comparison with a helium vapor pressure thermometer, and by the use of the boiling and triple points of hydrogen and nitrogen and the sublimation point of dry ice as fixed points.

The excitation and detection circuits are shown in Fig. 2. The modified van Zelst[10] bridge, isolated by the dotted lines of Fig. 3, constitutes the capacitive branch of the tank circuit of a 60 Mc/sec amplifier. The

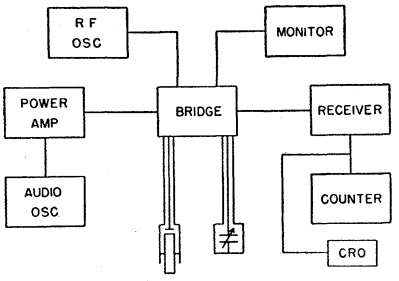

FIG. 2. Block diagram of circuitry.

[10] J. J. Zaalberg van Zelst, Philips Tech. Rev. 9, 357 (1947).

inductances L_1 and L_2 are in fact capacitances terminating quarter wave lines with characteristic impedance Z_0 so that, for example, $L_1=Z_0^2C_1'$. C_1' is the capacitance between driving plate and specimen; C_2' is a tunable capacitor by which the bridge is balanced. The bridge output is modulated by the variation of C_1' and detected by a Hallicrafter's model SX-62A communications receiver. This symmetric bridge network minimizes noise arising from random fluctuations in carrier amplitude and frequency.

Internal friction is measured by counting the number of cycles of specimen vibration occurring during free decay using a gated electronic counter. The inverse of the storage factor, Q^{-1}, is given by

$$Q^{-1}=\frac{\text{energy dissipated per cycle}}{2\pi \text{ energy stored per cycle}}=(1/\pi N)\ln(V_1/V_2), \quad (1)$$

where N is the number of cycles passing between voltage levels V_1 and V_2 which open and close the

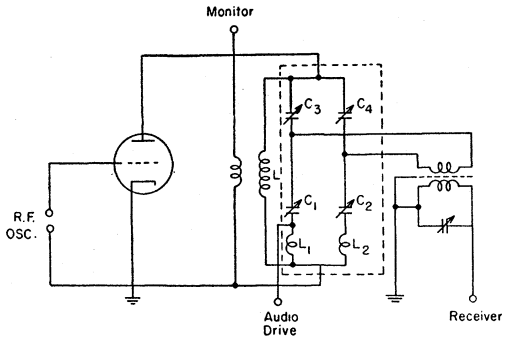

FIG. 3. Schematic diagram of bridge circuit.

counter gate. Calibration is provided by the use of precision RC elements to generate exponential waveforms with known decay times. All decay waveforms are displayed on an oscilloscope equipped with a triggered sweep.

Resonant frequencies are measured by counting the number of vibrations occurring during an accurately known time interval, determined by suitable gating pulses generated by interrupting a light beam with a pendulum.

Strain amplitudes are less than 10^{-7} and are determined by

$$\sigma_{\max}=2CV_0V_1/\pi nAEdQ^{-1}, \quad (2)$$

where $\sigma_{\max}$=maximum strain amplitude, C=capacity between specimen and end plate, V_0=dc component of driving voltage, V_1=ac component of driving voltage, n=number of harmonic excited, A=cross sectional area of specimen, E=Young's modulus of specimen, and, d=width of gap between driving plate and specimen.

The maximum displacement amplitude, D_0, of the

end of the specimen is given by:

$$D_0 = 2CV_0V_1L/\pi^2n^2AEdQ^{-1}, \quad (3)$$

where L is the length of the bar.

III. EXPERIMENTAL RESULTS

All the experimental data are presented in this section, detailed discussion and interpretation being deferred to the next section. The data are exhibited as plots of Q^{-1} versus temperature where Q^{-1} is given by Eq. (1). Only representative measured points are indicated; these curves are based on measurements made at intervals of 3°K. Measurements of Q^{-1} have a precision of 3% or better, except when otherwise stated. Resonant frequencies are determined with an accuracy of 0.01%.

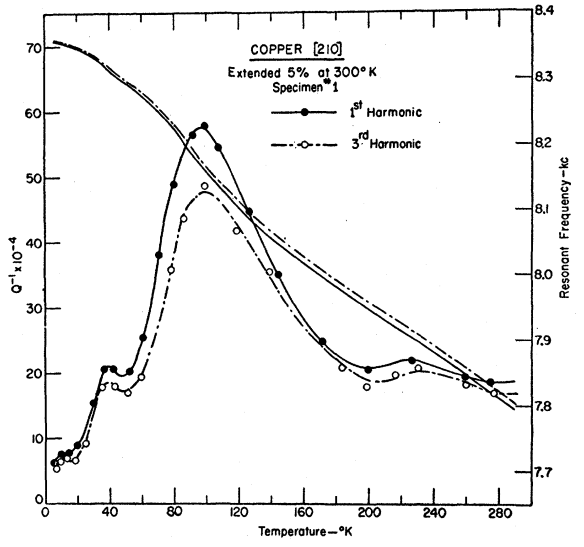

FIG. 4. Loss and resonant frequency vs temperature for Cu single-crystal specimen 1.

A. Face-Centered Cubic Metals and Alloys

1. Copper

The most extensive measurements to be reported have been made on copper. Both single and polycrystalline specimens have been prepared using A. S. & R. 99.999% spectrographic grade material. Single-crystal specimens, grown in graphite crucibles under vacuum by the Bridgman method, were stretched in an extensometer equipped to provide a stress-strain histogram.

Figure 4 summarizes the results of measurements made on single-crystal specimen 1 of axial orientation [210] extended 5% at 300°K. Both first and third harmonics were excited. The precision of Q^{-1} determined for the third harmonic is only 10% owing to the much lower displacement amplitude in this mode of vibration. In Fig. 4, the resonant frequencies measured for the third harmonic are divided by three for comparison

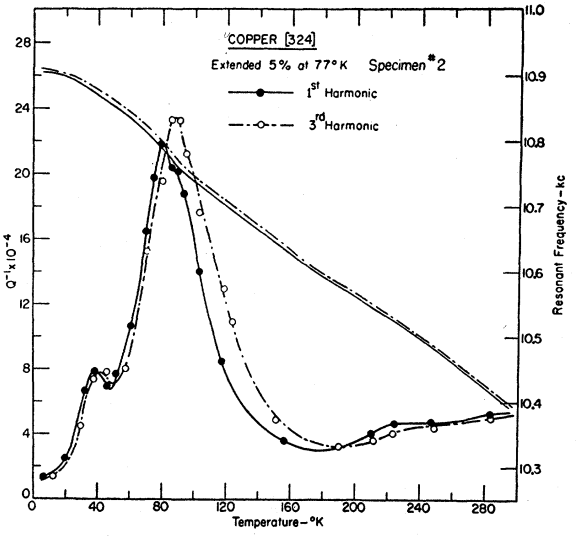

FIG. 5. Loss and resonant frequency vs temperature for Cu single-crystal specimen 2.

with the fundamental. Figure 5 exhibits similar results obtained on single-crystal specimen 2 of axial orientation [324] extended 5% while immersed in a liquid nitrogen bath at 77°K.

For both specimens 1 and 2 the deformation was carried into the second or linear stage of the work hardening curve characteristic of fcc pure metal single crystals,[11] the principal differences between the experiments being the crystal orientation and the temperature of deformation. A comparison of loss data for samples 1 and 2 (first harmonic only) is presented in Fig. 6, when Q^{-1} has been normalized by dividing by $Q_{\max}^{-1}$, the height of the major peak. This normalization procedure emphasizes the different behavior observed in these specimens. These experiments were motivated

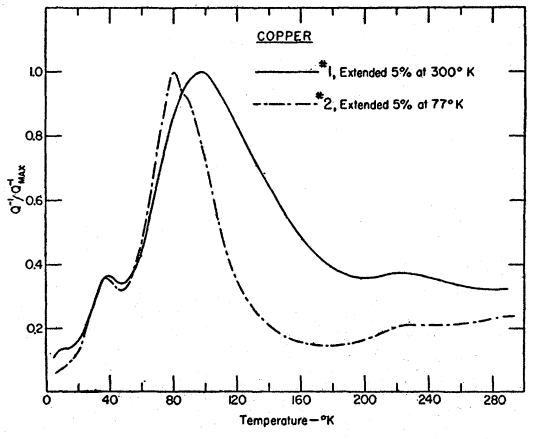

FIG. 6. Normalized comparison plot for first harmonic loss data for Cu specimens 1 and 2.

[11] A. Seeger, *Dislocations and Mechanical Properties of Crystals* (John Wiley & Sons, New York, 1957), p. 243.

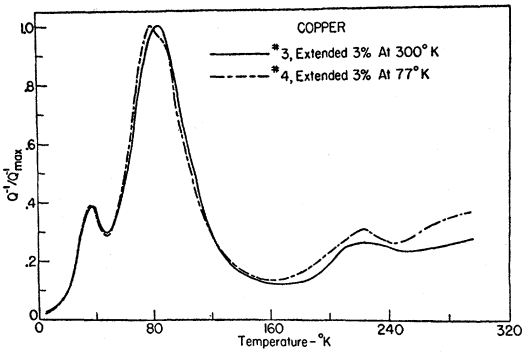

FIG. 7. Normalized comparison plot of first harmonic data for polycrystalline Cu specimens 3 and 4.

by the theoretical work of Seeger[12] on the temperature dependence of flow stress in fcc metals of low stacking fault energy; they will be discussed further below.

A similar set of measurements was made on polycrystalline copper specimens to ascertain further whether factors other than temperature of deformation were important. The samples were vacuum annealed for four hours at 600°C and were fully recrystallized prior to deformation. Sample 3 was extended 3% at 300°K, sample 4 was extended 3% at 77°K. Figure 7 presents the loss data for the fundamental mode in the two cases, normalized in accordance with the procedure used in Fig. 6 for the single-crystal data. Although qualitatively similar, the results suggest that other factors, such as orientation in the case of single crystals, and degree of deformation, can affect the position and shape of the peaks.

In order to test the effect of deformation rate, polycrystalline copper was pretreated as for samples 3 and 4 and then subjected to explosive shock. A photograph of the shot assembly is shown in Fig. 8. The sample was placed into a close fitting hole in a large block of commercial copper stock. The explosive generated a plane shock front of about 200-kilobars intensity incident parallel to the specimen axis. The guard block was later cut away and the specimen removed. As may be seen in Fig. 9, the loss curves are quite similar, but the minor peak is not as well resolved as in specimens deformed statically. This experiment was made possible by the kind cooperation of Dr. G. E. Duvall and Dr. G. R. Fowles of the Stanford Research Institute.

A summary of the essential features of the copper data is presented in Table I.

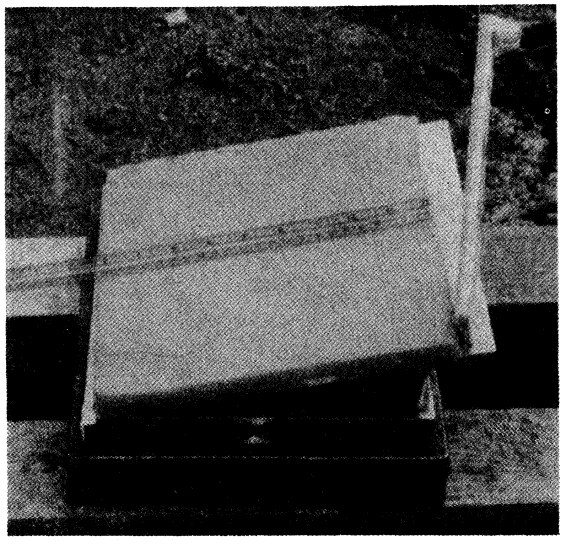

FIG. 8. Photograph of explosive shot assembly used in preparation of polycrystalline Cu specimen 5.

[12] A. Seeger, Phil. Mag. 46, 1194 (1955).

2. *Aluminum and Aluminum-Copper Alloys*

Because the general effects observed in single-crystal and polycrystalline copper were the same, only polycrystalline samples of aluminum and aluminum-copper alloys were studied. The pure sample was prepared by annealing 99.99% aluminum in vacuum for twelve hours at a temperature of 550°C. It was then extended 3% at 300°K. The loss data for this sample, number 6, are illustrated in Fig. 10, where they are compared with corresponding data on the same sample after a vacuum anneal of one hour at 190°C.

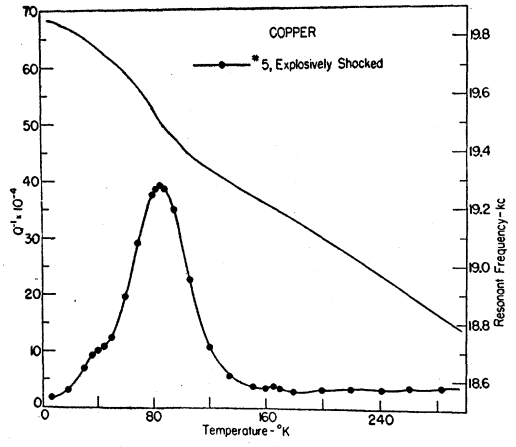

FIG. 9. Loss and resonant frequency vs temperature for polycrystalline copper specimen 5, subjected to explosive shock.

It is evident that the principal maximum is resolvable into two component peaks, one at 100°K and one at 128°K. In addition the small subsidiary peak at 24°K will be noted. It has recently been reported by Lax and Filson.[13]

Two alloy specimens were prepared by adding 0.25 at. % copper to a pure aluminum melt. These were then annealed for four hours at 500°C and water quenched. Both were immediately extended 3%, then one (specimen 8) was aged for one hour at 180°C prior to measurement; the other (specimen 7) was aged for

[13] E. Lax and D. H. Filson, Phys. Rev. 114, 1273 (1959).

TABLE I. Summary of copper data.

Specimen No.	Length	Description	Major peak T_{max}	Major peak Q_{max}^{-1}	Minor peak T_{max}	Minor peak Q_{max}^{-1}	Resonant frequency, $T=0°K$
1	20 cm	Single crystal [210] extended 5% at 300°K	96°K	57.5×10^{-4}	39°K	21.0×10^{-4}	8.356 kc/sec 1st harmonic
			100°K	47.5	40°K	18.6	25.074 kc/sec 3rd harmonic
2	20 cm	Single crystal [324] extended 5% at 77°K	79°K	21.9	38°K	7.8	10.906 kc/sec 1st harmonic
			87°K	23.5	42°K	7.8	37.730 kc/sec 3rd harmonic
3	20 cm	Polycrystal extended 3% at 300°K	84°K	24.1	38°K	9.5	9.631 kc/sec
4	20 cm	Polycrystal extended 3% at 77°K	79°K	24.3	37°K	9.4	9.003 kc/sec
5	10 cm	Polycrystal explosively shocked	86°K	39.4	unresolved		19.866 kc/sec

one week at room temperature. The results, presented in Fig. 10, show that all peak structure observed in the pure aluminum has been eradicated, Q^{-1} being only about 10^{-6} at low temperature

B. Body-Centered Cubic Metals and Alloys

The plastic properties of bcc metals are known to be strongly affected by their interstitial impurity content. To minimize the effects of dislocation pinning by interstitials, a particular effort was made to secure pure materials. The results of analysis for interstitial impurities in all bcc metals and alloys studied are summarized in Table II

1. Iron

Specimen 9 was cut from an ingot of annealed vacuum melted iron. It was 10 cm long as were all samples of the bcc metals and alloys used. The specimen bar was reduced in area 8% by swaging at room temperature prior to measurement, the results of which are shown in Fig. 11 where they are compared to those obtained on the same sample after an anneal of 4 hours *in vacuo* at 850°C.

Zone refined iron was obtained through the courtesy of Dr. J. W. Halley, Dr. K. L. Fetters, and Dr. G. W. Rengstorff; it was prepared by the latter at the Batelle Memorial Institute. An ingot measuring $1\frac{3}{4}$ in. $\times 1\frac{1}{4}$ in. $\times\frac{3}{4}$ in. was reduced by rolling and swaging to produce specimen 10 which was measured in the as-deformed condition. See Fig. 11. No intermediate annealing was required for this cold reduction.

TABLE II. Analysis for interstitial impurities in bcc metals and alloys (ppm by weight).

Specimen	O	N	H	C
#9; vacuum melted iron	9	37	a	18
#10; zone refined iron	17	<2	<0.2	10
#11; niobium	210	28	4	32
#12; β brass	22	3	2	a

[a] Not determined.

In neither specimen is there any evidence of a relaxation peak occurring in the temperature range covered. There is no theoretical indication that Bordoni peaks might be expected at higher temperatures in iron. The results are atypical, however, in that the loss increases with decreasing temperature, attaining a maximum value at about 50°K and maintaining that value to the lowest temperature reached. Evidence that dislocations do not contribute to this low-temperature loss, and may in fact impede the mechanism responsible, is provided by the fact that the loss is highest in the annealed specimen. This behavior is not understood but is probably related to the fact that the material is ferromagnetic.

2. Niobium

The possible complications of ferromagnetic materials was avoided by a study of niobium. A niobium specimen, number 11, kindly supplied by Dr. R. J. Wasilewski of E. I. du Pont de Nemours and Company, was prepared by cold swaging to a total reduction in

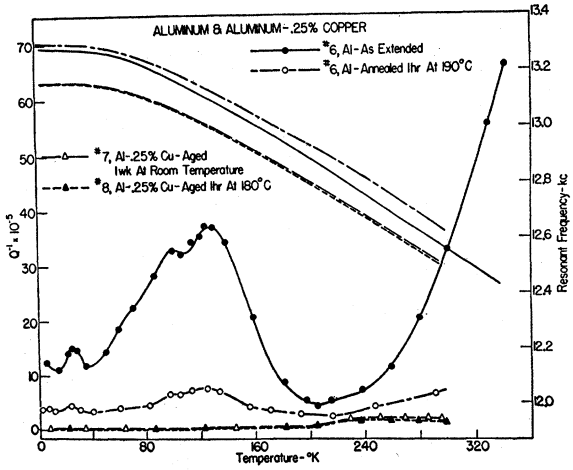

FIG. 10. Loss and resonant frequency vs temperature for polycrystalline pure aluminum specimen 6, and for polycrystalline Al—0.25 at. % Cu specimens 7 and 8.

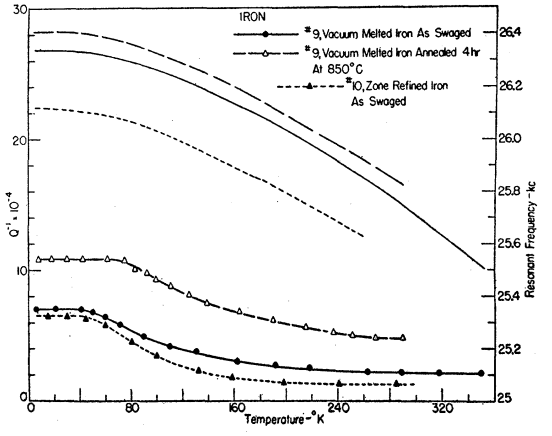

FIG. 11. Loss and resonant frequency vs temperature for vacuum melted Fe specimen 9 and zone refined Fe specimen 10, both polycrystalline.

area of 60%. It was measured in the as-deformed condition with the results illustrated in Fig. 12. It was then vacuum annealed for two hours at 300°C and remeasured. The loss peak observed initially at 173°K was completely removed by the anneal. The recrystallization temperature of niobium is known,[14] however, to be of the order of 900°C. This result is clearly not consistent with the annealing characteristics of the Bordoni peaks observed in fcc metals.

We believe that this peak is not a Bordoni type, but is associated with the presence of hydrogen in the specimen. Further discussion of this point is reserved to Sec. VI.

3. β Brass

The study of bcc systems was further extended by measurements on β brass. Specimen 12 was prepared using spectrographic grade copper and zinc and showed upon analysis a composition of 51.61 wt % copper and 48.39 wt % zinc. Homogeneity of the β phase was established by x-ray analysis.

It was extended 2.5% at 300°K; the results of measurement are illustrated in Fig. 13. The specimen was then annealed in argon for two hours at 350°C and remeasured. It will be noted that the rather complex peak structure observed at 220°K and 300°K was modified but not removed by this treatment. A small peak observed at 138°K in the specimen as originally deformed was removed by annealing however. The temperature dependence of the resonant frequency of the specimen is related to the well-known anomaly in the temperature dependence of the elastic constants in β-phase alloys.[15]

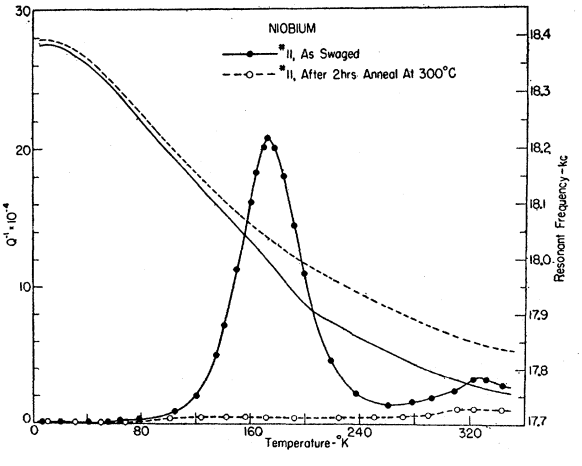

FIG. 12. Loss and resonant frequency vs temperature for polycrystalline Nb specimen 11.

[14] R. J. Wasilewski, E. I. du Pont de Nemours and Company (private communication).

IV. DISCUSSION

We discuss here the experimental evidence leading to a proposed interpretation of the Bordoni peaks.

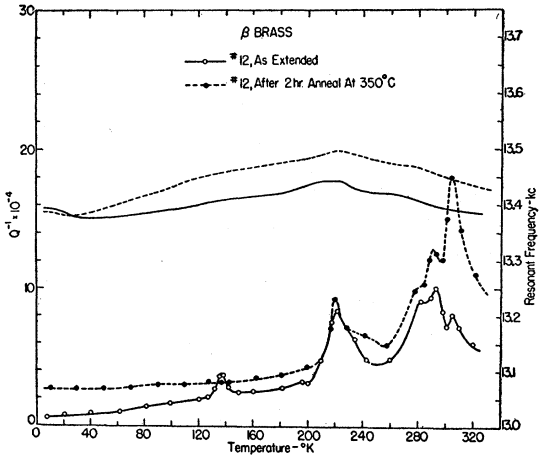

FIG. 13. Loss and resonant frequency vs temperature for polycrystalline β-brass specimen 12.

The principal experimental facts associating dislocations with such internal friction maxima are, as outlined in the introduction, that they occur only in plastically deformed metals and are stable until the dislocation density is reduced by recrystallization.

The mechanism of dislocation relaxation developed by Seeger and others[16–18] envisages the formation of double kinks or loops in otherwise straight dislocation lines. Activation energies are calculated in terms of the Peierls stress and other intrinsic dislocation parameters, and are thus insensitive to degree of deformation and dilute impurity content as required by observation.

The Seeger theory must, however, be examined in the light of two principal experimental results of the

[15] C. Zener, Phys. Rev. 71, 846 (1947).
[16] A. Seeger, Phil. Mag. 1, 651 (1956).
[17] A. Seeger, H. Donth, and P. Phaff, Discussions Faraday Soc. 23, 19 (1957).
[18] H. Donth, Z. Physik 149, 111 (1957).

present work. The first is the apparent absence of Bordoni peaks in pure bcc metals. Seeger's mechanism rests upon two basic dislocation parameters, the line tension and the Peierls stress. Calculated activation energies are roughly proportional to the square root of their product and as such would not be expected to differ markedly between bcc and fcc metals.

The suppression of all peak structure in the strain aged Al-Cu alloys is the second experimental fact to be considered. The metallographic studies of Wilsdorf and Kuhlmann-Wilsdorf[19] indicate that precipitation of θ-phase Al-Cu occurs only on edge dislocations. These results suggest that pure screw dislocations are not immobilized by precipitation, yet do not contribute to dislocation relaxation. The Seeger mechanism predicts that both screw and edge dislocations contribute.

The above conclusions lead first to a search for significant differences in dislocation configuration between fcc and bcc lattices. One such difference is in the formation of partial dislocations. The planes and directions of slip in the fcc lattice are (111) and [110], respectively, and the dissociation reaction[20]

$$\tfrac{1}{2}a[110] \rightarrow \tfrac{1}{6}a[211]+\tfrac{1}{6}a[12\bar{1}] \qquad (4)$$

is energetically favorable. Equation (4) describes the dissociation of a complete dislocation into a pair of Shockley partials with Burgers vectors of equal magnitude. Their equilibrium separation is determined by the surface energy of the stacking fault joining them. For the bcc case the principal planes and directions of slip are (110) and [111] and no dissociation is possible. The case of slip on (211) planes where the asymmetric reaction

$$\tfrac{1}{2}a[111] \rightarrow \tfrac{1}{3}a[111]+\tfrac{1}{6}a[111] \qquad (5)$$

can occur will be considered below.

Secondly, we are led to search for significant differences between edge and screw dislocations. One such difference is in the interaction of point defects with dislocations, as is confirmed for example by the strain aging experiment itself. An undissociated screw dislocation does not interact with such defects because, to first approximation, the stress field is pure shear. An edge dislocation, on the other hand, can interact strongly with a point defect through its dilatational field.[21]

We now consider qualitatively the interaction between a pair of dissociated partials in a fcc lattice and a point defect, resolving the Burgers vector of each partial into an edge and a screw component. We consider only the edge component in accordance with the remarks of the previous paragraph. Implicit here is the assumption of superposition of elastic fields generally employed in the calculation of dislocation stress fields using isotropic elasticity theory.

When a pure screw dissociates, the partials have edge components which are equal in magnitude but opposite in sign. Consider a defect fixed at a point above the glide plane. The dislocation will assume a stable position such that one partial lies immediately below it, by virtue of the interaction of the dilatational field of the edge component with the volume change introduced by the defect. The edge component of the other partial, being opposite in sign, will be repelled by the defect, and only one equilibrium configuration is possible for dissociated screws. On the other hand, for a dissociated pure edge dislocation, the partials formed will have edge components equal both in magnitude and sign. Hence, two energetically symmetric configurations can occur.

It is clear now that thermally activated transition of a dissociated edge dislocation from one stable configuration to another provides a mechanism of damping which does not occur for screws. For the case of bcc lattices the reaction of Eq. (5), if it occurs, would also be expected to yield two stable positions for a general line orientation. However, the edge components, though of the same sign, will have magnitudes in the ratio 2:1. The resulting asymmetry in the equilibrium configurations considerably reduces the effectiveness of dislocation hopping as a loss mechanism.

Hence, the interaction of dislocations with point defects provides a damping mechanism which exhibits the required difference between edge and screw dislocations on the one hand and fcc and bcc metals on the other. We therefore elaborate it into a semi-quantitative theory of the Bordoni peaks in the next section. Before doing so, however, we examine the evidence which bears upon the selection of the point defect or defects responsible.

First we consider impurities. It has been established[2,5] that dilute ($<1\%$) impurities in solid solution can lower the amplitude of both peaks and background but have little or no effect on the maximum loss temperature. This relative independence of peak position of impurity content suggests that they play only a secondary role.

We are thus led to consider intrinsic point defects. The choices are interstitials, vacancies or possibly complexes thereof. Interstitials can probably be ruled out on the basis of the fact that they are not produced in significant numbers during plastic deformation. Evidence for this is available from data on low-temperature annealing of resistivity in which the annealing steps observed in irradiated copper and attributed to interstitial migration are not observed in cold-worked copper.[22]

[19] H. Wilsdorf and D. Kuhlmann-Wilsdorf, *Report of the Bristol Conference on Defects in Crystalline Solids, July, 1954* (The Physical Society, London, 1955), p. 175.

[20] W. T. Read, Jr., *Dislocations in Crystals* (McGraw-Hill Book Company, Inc., New York, 1953), p. 92.

[21] A. H. Cottrell, *Dislocations and Plastic Flow in Crystals* (Clarendon Press, Oxford, 1953), p. 56.

[22] J. S. Koehler, J. W. Henderson, and J. H. Bredt, *Dislocations and Mechanical Properties of Crystals* (John Wiley & Sons, New York, 1957), p. 587.

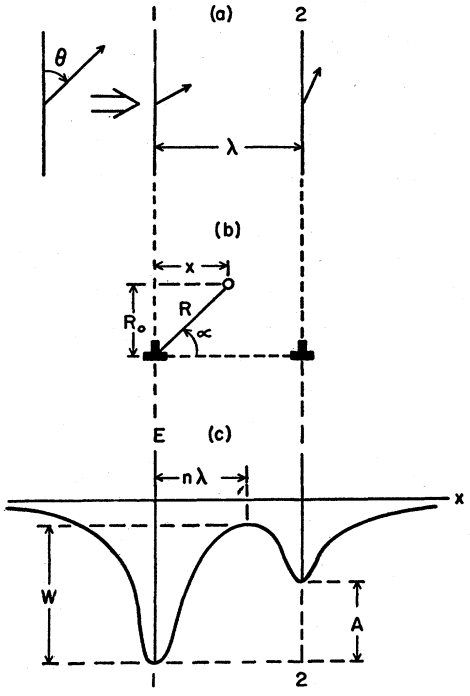

FIG. 14. Schematic representation of the dissociation of a complete dislocation into partials, (a) viewed from above the glide plane; and (b) viewed along the glide plane. The shape of the double potential well for interaction between split partials and a point defect is shown in (c).

We are left with vacancies as the simplest point defects likely to be responsible for the Bordoni peaks. It is well established, again by annealing of resistivity measurements, that vacancies are produced in significant numbers by plastic deformation. There is substantial theoretical evidence[23] as well for their generation on the glide planes of moving dislocations during the course of plastic deformation.

V. FORMAL DEVELOPMENT OF THE MODEL

Here we present a semiquantitative development of the ideas put forth in the previous section. The dissociation reaction given by Eq. (4) describing the formation of Shockley partials in fcc metals is represented schematically in Fig. 14(a). Bearing in mind the remarks of the previous section we write for the interaction energy $U_1(R,\alpha)$ between a vacancy and partial 1 of Fig. 14(a), using the well-known formula due to Cottrell[21]

$$U_1(R,\alpha)=A(\sin\alpha)/R, \tag{6}$$

where

$$A=\tfrac{4}{3}[(1+\nu)/(1-\nu)]\mu_E b_1 \epsilon r^3. \tag{7}$$

Here ν is Poisson's ratio, μ_E is the elastic shear modulus, b_1 is the magnitude of the edge component of the Burgers vector of the partial, r is the atom radius of the solvent, and ϵ is given by $r'=(1+\epsilon)r$ where r' is the effective radius of the vacancy. R and α are the polar coordinates illustrated in Fig. 14(b).

Since the model envisages the thermally activated motion of a dislocation about a vacancy which is fixed at a distance R_0 above the glide plane, it is convenient to rewrite Eq. (6) as

$$U_1(x')=\frac{A}{R_0}\frac{1}{1+x'^2}, \tag{8}$$

where $x'=x/R_0$ and x is the horizontal displacement of the vacancy from partial 1. A similar expression may be written for $U_2(x')$ with b_1 replaced by b_2, the magnitude of the edge component of partial 2 in Fig. 14(a), and x' replaced by $(\lambda'-x')$. Here $\lambda'=\lambda/R_0$ where λ is the spacing between partials. The total interaction is given by the sum

$$U_{1,2}(x')=U_1(x')+U_2(x')$$

$$=\frac{A}{R_0}\left[\frac{1}{1+x'^2}+\frac{\mathrm{K}}{1+(\lambda'-x')^2}\right], \tag{9}$$

where $\mathrm{K}=b_2/b_1$.

In general the interaction will lead to an asymmetric double potential well as shown in Fig. 14(c). Since in the rate calculation to follow it will be shown that asymmetric configurations do not contribute appreciably to the relaxation strength, we now calculate the activation energy W_0 for the symmetric case only. Here $\theta=90°$ in Fig. 14(a) corresponding to a dissociated pure edge dislocation. For the symmetric case $\mathrm{K}=1$ and

$$W_0=U_{1,2}(x'=\lambda'/2)-U_{1,2}(x'=0)$$

$$=\frac{A}{R_0}\left[\frac{2}{1+(\lambda'/2)^2}-\left(1+\frac{1}{1+\lambda'^2}\right)\right]. \tag{10}$$

The separation of the partials, λ, is given by[24]

$$\lambda=\lambda' R_0=\frac{\mu_E b^2}{8\pi E_f}\frac{(2-\nu)}{(1-\nu)}\left(1-\frac{2\nu}{2-\nu}\cos 2\theta\right), \tag{11}$$

where b is the magnitude of the Burgers vector of a Shockley partial and E_f is the stacking fault energy.

The only other parameter requiring explicit evaluation is ϵ. On the basis of thermodynamic arguments it has been shown[25] that for vacancies

$$\Delta V^*/V=(\gamma_G-\tfrac{1}{3})^{-1}, \tag{12}$$

where $\Delta V^*/V$ is the fractional change in volume upon formation of a vacancy and γ_G is the Gruneisen constant. Hence

$$\epsilon=-\tfrac{1}{3}(1-\Delta V^*/V)=-\tfrac{1}{3}[1-(\gamma_G-\tfrac{1}{3})^{-1}]. \tag{13}$$

[23] F. Seitz, *Advances in Physics*, edited by N. F. Mott (Taylor and Francis, Ltd., London, 1952), Vol. 1, p. 43.

[24] See reference 20, p. 131.

[25] A. W. Lawson, S. A. Rice, R. D. Corneliussen, and N. H. Nachtrieb, J. Chem. Phys. (to be published).

Equations (7), (10), (11), and (13) now permit calculation of activation energies W_0 in terms of known parameters. The results for copper and aluminum are presented in Table III. The two choices for R_0, $R_0=\frac{1}{4}a[111]$ and $R_0=\frac{3}{4}a[111]$ represent situations where the interacting vacancy is one atom plane or two atom planes above the glide plane, respectively. It should be noted that the second value of R_0 gives a negative activation energy for the case of aluminum, i.e., no central maximum. The numerical values given are in reasonable accord with experiment.

In this development, no account has been taken of the contribution of the stacking fault to the stress fields of the pair of partials. In our model, we regard a partial dislocation which terminates a semi-infinite plane of stacking fault as being acted upon by a line source of shear coincident with the dislocation line and generated by the fault. For a pair of partials bounding a ribbon of fault, two such line sources would be present, their direction and magnitude being such as to balance the effective repulsive force between the two partials. Following the analytical procedure of Love,[26] it may be shown that the stress field surrounding a line source of shear acting within a homogeneous medium of infinite extent is a pure shear field. Hence, to first order no contribution to the dilatational fields of the partials is expected; consequently there will be no correction to the interaction energy arising from the presence of the fault. In our approximate formulation we have consistently disregarded the second-order compression associated with a pure shear.

We turn now to a calculation of the loss Q^{-1} starting with the general potential well illustrated in Fig. 14(c). We write

$$N_1(t)=N_1^{(0)}+N_1'e^{j\omega t}, \tag{14}$$

$$N_2(t)=N_2^{(0)}+N_2'e^{j\omega t}, \tag{15}$$

TABLE III. Results for copper and aluminum

	Copper	Aluminum
a	3.62×10^{-8} cm	4.05×10^{-8} cm
μ_E	3.05×10^{11} dyne/cm^2	2.44×10^{11} dyne/cm^2
ν	0.33	0.33
b	$\frac{1}{2}a[211]=1.48\times10^{-8}$ cm	$\frac{1}{2}a[211]=1.67\times10^{-8}$ cm
E_f	40 erg/cm^2	200 erg/cm^2
θ	90°	90°
λ	$6.40a=23.2\times10^{-8}$ cm	$1.15a=4.66\times10^{-8}$ cm
b_1	$b\cos30°=1.28\times10^{-8}$ cm	$b\cos30°=1.44\times10^{-8}$ cm
r	$\frac{1}{4}a[110]=1.28\times10^{-8}$ cm	$\frac{1}{4}a[110]=1.44\times10^{-8}$ cm
γ_G	1.96	2.17
ϵ	−0.202	−0.213
R_0	$\frac{1}{4}a[111]=1.57\times10^{-8}$ cm	$\frac{1}{4}a[1\bar{1}1]=1.75\times10^{-8}$ cm
λ'	14.8	2.66
W_0	0.168 ev	0.085 ev
R_0	$\frac{3}{4}a[111]=4.71\times10^{-8}$ cm	$\frac{3}{4}a[111]=5.25\times10^{-8}$ cm
λ'	4.93	0.89
W_0	0.045 ev	−0.023 ev

[26] A. E. H. Love, *The Mathematical Theory of Elasticity* (Dover Publications, New York, 1944), 4th ed., p. 204.

where $N_1(t)$ and $N_2(t)$ are the number per unit volume of configurations in well 1 and well 2, respectively, at time t. $N_1^{(0)}$ and $N_2^{(0)}$ are their equilibrium populations under zero external stress; N_1' and N_2' represent the time dependent deviations in population. Using standard rate theory as applied by Hall[27] we obtain

$$N_2'-N_1'=\frac{N_0\Delta E_0}{2kT}B(T)\frac{1}{1+j(\omega/\bar{\omega})}, \tag{16}$$

where

$$B(T)=4[2+(\gamma_1/\gamma_2)e^{-A/kT}+(\gamma_2/\gamma_1)e^{A/kT}]^{-1}, \tag{17}$$

and where

$$\bar{\omega}=\gamma_1e^{-W/kT}+\gamma_2e^{-(W-A)/kT}. \tag{18}$$

Here γ_1 and γ_2 are attempt frequencies characteristic of well 1 and well 2, respectively; W and A are the barrier heights shown in Fig. 14(c). Also $N_0=N_1^{(0)}+N_2^{(0)}$ is the total number of appropriate dislocation-vacancy configurations per unit volume. Further ΔE_0 is the change in the energy difference A between wells 1 and 2 resulting from the application of an external shear stress τ_0. For a sinusoidal stress we have $\Delta E=\Delta E_0e^{j\omega t}$ corresponding to $\tau=\tau_0e^{j\omega t}$.

Now the maximum plastic strain per unit volume is

$$\sigma_{0p}=(N_2'-N_1')Sb_0=\tfrac{1}{2}(N_2'-N_1')b_0\lambda l, \tag{19}$$

where S is the area swept out on the glide plane when an activated jump occurs and b_0 is the magnitude of the Burgers vector of the undissociated dislocation since the dislocation pair moves as a unit. We have set $S=\frac{1}{2}\lambda l$ since the dislocation pair moves an average distance $\lambda/2$ between pinning points spaced a distance l apart. The evaluation of l will be discussed in the next section. Further, ΔE_0 equals the force per unit length τ_0b_0 on the dislocation pair multiplied by the length l of dislocation involved and the average distance $\lambda/2$ through which it moves. Thus we have

$$\Delta E_0=\tfrac{1}{2}\tau_0b_0\lambda l=\tfrac{1}{2}b_0\lambda l\mu_E\sigma_{0E}, \tag{20}$$

where σ_{0E} is the maximum elastic strain. We now combine Eqs. (16), (19), and (20) to obtain

$$\frac{\Delta\mu}{\mu_E}=\frac{\mu_E-\mu(\omega)}{\mu_E}=\frac{\mathrm{Re}\,(\sigma_{0p})}{\sigma_{0E}}$$

$$=\frac{N_0l^2b_0^2\lambda^2\mu_E}{8kT}B(T)\frac{1}{1+(\omega/\bar{\omega})^2}, \tag{21}$$

and

$$Q^{-1}(\omega)=\frac{\mathrm{Im}\,(\sigma_{0p})}{\sigma_{0E}}=\frac{N_0l^2b_0^2\lambda^2\mu_E}{8kT}B(T)\frac{(\omega/\bar{\omega})}{1+(\omega/\bar{\omega})^2}. \tag{22}$$

Equation (17) shows that for $A>kT$ the relaxation strength goes to zero as $e^{-A/kT}$. It is now clear why only dissociated pure edge dislocations for which $A=0$ can contribute to relaxation. Detailed analysis for the case

[27] L. Hall, Phys. Rev. 73, 775 (1958).

TABLE IV. Comparison of theory and experiment for copper.

Configuration	ω-sec^{-1} (excitation frequency)	ω_0-sec^{-1} (calculated)	W_0-ev (calculated)	T_{max} (calculated)	T_{max} (observed)
Single vacancy $R_0=\frac{1}{4}a[111]$	6×10^4	7.8×10^{11}	0.168	120°K	85°K
Single vacancy $R_0=\frac{3}{4}a[111]$	6×10^4	1.5×10^{11}	0.045	36°K	40°K
Divacancies $R_0=\frac{1}{4}a[111]$	6×10^4	1.1×10^{12}	0.336	234°K	220°K

of copper shows that a deviation of 15° from pure edge orientation reduces the relaxation strength by a factor of ten. Specializing again to the case of pure edge dislocations we have $B(T)=1$ and

$$Q_{max}^{-1}=N_0l^2a^2\lambda^2\mu_E/32kT_{max}, \quad (23)$$

where $a=\sqrt{2}b_0$ is the length of the cube edge in the fcc unit cell.

To calculate the attempt frequency we note that Eq. (9) may be expanded about the point $x'=0$ to give

$$U_{1,2}(x')=(A/R_0)(1-x'^2+\cdots), \quad (24)$$

from which we obtain the force constant

$$k=-2A/R_0^3. \quad (25)$$

It should be recalled that A is negative since ϵ is negative; hence k is a positive quantity. For the effective mass of a length l of extended dislocation we take

$$m=\rho b_0^2 l, \quad (26)$$

when ρ is the density of the material. The attempt frequency ω_0 is then

$$\omega_0=2\gamma_1=2(k/m)^{\frac{1}{2}} \quad (27)$$

for the symmetric case.

VI. CONCLUSION AND SUMMARY

In this section, we complete the quantitative comparison of the above model with experiment. We begin by making the following tentative assignment of the observed peaks in copper, using Table III as a guide:

1. The major peak ($T_{max}\cong85$°K), is associated with configurations in which the vacancy is one atom plane above the glide plane, i.e., $R_0=\frac{1}{4}a[111]$.
2. The minor peak ($T_{max}\cong40$°K), is associated with configurations in which the vacancy in two atom planes above the glide plane, i.e., $R_0=\frac{3}{4}a[111]$.
3. A higher temperature peak ($T_{max}\cong220$°K), is associated with pinning of dislocation loops by vacancy pairs.

To test this assignment quantitatively we must first assign a value to l, the effective length of dislocation involved in an activated transition of the type considered. For the major peak in copper we have measured $Q_{max}^{-1}\cong2\times10^{-3}$ at $T_{max}\cong85$°K. Using these values, in Eq. (23), together with other known parameters for copper, we find $N_0l^2\cong30$ cm^{-1}. If we assume that vacancies are the only pinning points which determine l, we have $N_0=L_{eff}/l$, where L_{eff} is the density of dislocations sufficiently close to edge orientation to contribute to relaxation. We estimate $L_{eff}\cong1/10L$, where L is the total dislocation density. This estimate assumes that dislocations are randomly oriented and that only those within about 15° of pure edge orientation contribute appreciably. We estimate[28] that $L\cong10^{11}$ cm^{-2}, from which $lL_{eff}\cong30$ cm^{-1}, or $l\cong3\times10^{-9}$ cm, which is clearly too small. We are thus led to consider vacancies as secondary in this regard; the principal factor determining L appears to be the mean distance between dislocation nodes. We set $l^2=L^{-1}$, from which $l=3\times10^{-6}$ cm, or about a hundred atom spacings. The possibility of pinning of dislocations by impurities will be discussed below.

The use of the numerical estimate for l given above, together with Eqs. (7), (25), (26), and (27), enables us to calculate attempt frequencies ω_0. The values of ω_0 so calculated, given in Table IV, together with calculated activation energies, permit us to compute the temperature T_{max} at which loss maxima should occur for the dislocation-vacancy configurations considered. The theoretical values of T_{max} are presented in Table IV, where they are compared with experimentally observed T_{max} in accordance with the scheme of identification assumed above. We have taken both the activation energy and the force constant for the divacancy configuration to be twice the calculated values for a single vacancy one atom plane above the glide plane. We believe that the comparison with experiment summarized in Table IV is more reasonable than a direct comparison of activation energies and of attempt frequencies, since the experimental determination of these parameters separately is rather uncertain.

Examination of Table IV suggests that the dislocation pressure acting on a vacancy in the nearest plane position has been overestimated by about 50%; the calculated activation energy and associated T_{max} are

[28] L. M. Clareborough, M. E. Hargreaves, and G. W. West, Proc. Roy. Soc. (London) **A232**, 252 (1955).

too high. This result is not surprising. Our simple model takes no account of the stress relaxation which must occur at the core of a dislocation. Furthermore, on the basis of the model, the energy difference between a vacancy-first plane and a vacancy-second plane configuration is about 0.1 ev. If this result were in fact correct, only about 2% of the vacancies would occupy second plane sites in thermal equilibrium at room temperature. Thus, the 40°K peak would not be observed. If, however, we reduce the energy difference to 0.05 ev, in accord with the estimated error in pressure, then roughly 15% of the vacancies will occupy second plane sites in thermal equilibrium at 300°K. Equation (23) then indicates that the ratio of $Q_{\max}^{-1}$ (minor peak) to $Q_{\max}^{-1}$ (major peak) would be about 0.3, in good accord with observations, if we regard the distribution of vacancies as frozen in at lower temperatures in accordance with annealing of resistivity measurements.[22]

The rather close agreement between theory and experiment for the divacancy configuration probably results from two compensating errors, namely an overestimate of the pressure and an underestimate of the volume of relaxation.

The theory predicts a third peak in copper corresponding to vacancy-third plane configurations with an activation energy of 0.017 ev. In only one case (specimen 1—Fig. 4) does it appear that such a peak may have been resolved at about 15°K. In general the occupation of this state will probably be too low to permit resolution of the corresponding peak.

Proceeding as before, we propose the following assignment scheme for aluminum:

1. The minor peak ($T_{\max}\cong 24$°K) is associated with single vacancy-first plane configurations.
2. The complex major peak ($T_{\max}\sim 100$°K) is associated with divacancies.

This appears to be the only scheme consistent with the calculations of Table III; there is no double minimum in the potential for single vacancy-second plane configurations. The high stacking fault energy[29] of aluminum makes the quantitative application of our simple model very uncertain. A more accurate theory might alter the assignment, since the results are quite sensitive to variation of λ, the separation of partials, when this parameter is small.

One important point to note, however, is that the relaxation strengths in aluminum are generally an order of magnitude lower than in comparably pretreated copper, in accord with Eq. (23) which predicts that $Q_{\max}^{-1}$ varies with λ^2.

The sharp rise in the loss for pure aluminum at about 250°K is probably associated with the onset of a breakaway mechanism of dislocation damping.[30] The rise in Q^{-1} at helium temperature does not appear to be due to a peak in this range.

We have been led to consider vacancies as the source of the interaction for the reasons given in the discussion. There is, however, no *a priori* reason for excluding impurities as a source. We can only suggest that, granting the validity of the model, impurities play a secondary role. They may serve, for example, to broaden the peaks either by contributing directly to relaxation with activation energies characteristic of their size factors or indirectly by close association with a vacancy pinning point. Experiments performed at higher excitation frequencies, using very pure host material, selectivity doped with impurities having size factors in the range 0.03–0.05, might resolve impurity peaks.

In evaluating the data on bcc systems we must consider the question of interstitial pinning of dislocations in detail. The total C and N content of the zone refined iron specimen is of the order of one part in 10^5. Assuming a dislocation density L of 10^{11} we find that l_0, the average distance between interstitial pinning points, is 10^{-6} cm or about 50 atom distances. This result is based on the assumption that all interstitial impurity reaches dislocation lines. It can be shown, using a loop length distribution function due to Koehler,[31] that the fraction α of the total dislocation density which is present in the form of free loops of length βl_0 or longer is

$$\alpha=\int_{\beta l_0}^{\infty}\frac{l}{l_0^2}e^{-l/l_0}dl=[1+\beta]e^{-\beta}. \tag{28}$$

Applying this result we find that about 10% of the total density can be expected to be present as loops of length $4l_0$ or longer; this is 200 atom spacings in the case of our zone refined iron. We therefore conclude that enough free length of dislocation is present to permit the Seeger mechanism to operate and that a corresponding peak should have been resolved, in contradiction to experiment. Although we regard our estimate of l_0 as a minimum value, there is no doubt that it would be desirable to study specimens of still higher purity when available.

The mechanism presented in this paper predicts a Bordoni peak in β brass since, in this material, we expect to find symmetric dislocation pairs separated by antiphase domain boundaries. The small peak observed at 138°K in the as-deformed specimen, which was removed by anneal, is the only one of those found which could be considered a Bordoni type; its identification as such is very uncertain, however, in view of the rich variety of effects which are observed in internal friction studies in β brass at higher temperatures.[32] We offer

[29] P. R. Thornton and P. B. Hirsch, Phil. Mag. 3, 738 (1958).
[30] W. P. Mason, *Physical Acoustics and the Properties of Solids* (D. van Nostrand and Company, Inc., Princeton, 1958), p. 231.
[31] J. S. Koehler, *Imperfections in Nearly Perfect Crystals* (John Wiley & Sons, New York, 1952), p. 197.
[32] L. M. Clareborough, Acta Met. 5, 413 (1957).

no explanation of the complex peak structure observed at 220°K and 300°K in β brass.

We believe that the pronounced peak in niobium observed at 173°K is associated with the presence of hydrogen in the deformed material. The situation seems to be analogous to that observed by Weiner and Gensamer[33] in hydrogen charged iron. They observe peaks at 50°K and 105°K, the first being attributed to stress induced diffusion of interstitial hydrogen, the second to the interaction of hydrogen with dislocations. Upon aging, the second peak initially grows at the expense of the first, then decays with further aging, leaving neither peak in evidence. In niobium, a very small hump is observed in the loss of the cold-worked specimen at about 70°K, which is tentatively identified with diffusion of interstitial hydrogen; the major peak at 173°K is thought to correspond to the 105°K peak in iron. The absence of all peak structure in the specimen after the anneal is taken to be indicative of the overaged condition, where interstitial saturation of the dislocations is complete. Our niobium specimen contained about 0.04 at. % hydrogen. Our failure to observe the hydrogen peaks in iron is attributable to a much lower content, being less than 0.001 at. % in the case of zone refined iron. Analogous phenomena have been observed by Ke[34] for the case of nitrogen in iron. Our conclusion is tentative; further experimentation is required to settle the point. If it is correct, the peak observed in niobium is clearly not of the Bordoni type, since its occurrence would be dependent upon both hydrogen content and deformation.

The room-temperature vs low-temperature deformation experiments in copper were undertaken since it was considered that a substantial change in the edge to screw ratio in the dislocation density might occur. This conclusion is based on a theory of the temperature dependence of flow stress in fcc metals of low stacking fault energy due to Seeger.[12] Although some differences are observed, their significance is difficult to assess. We regard the results as being consistent with our view that only edge components contribute to dislocation relaxation. The unusually high loss and high T_{max} of specimen 1 is not understood but may be associated with the fact that the [210] orientation is particularly favorable to double slip.

The theory developed here, in contrast to that of Seeger, does not depend on the Peierls stress. The problem of the strain amplitude dependence of the activation energy, which is predicted by Seeger but not observed,[2,5,6] can thus be resolved. The necessity of assigning rather high values, of order $10^{-3}\,\mu_E$, to the Peierls stress can also be avoided.

The relaxation strengths of the Bordoni peaks in copper are known to saturate at about 2% pre-strain.[2] This can be accounted for on the basis of the Seeger theory only if the density of dislocations lying in close-packed directions becomes constant for strains beyond this level. The total dislocation density is known, however, to be a linear function of strain to much higher levels.[28] The theory presented here predicts that Q_{max}^{-1} will be related to the pre-strain through the parameter $N_0 l^2$. If we take $l^2 \cong L^{-1} = (10 L_{eff})^{-1}$, and $N_0 \cong \eta_0 L_{eff}$, where η_0 is the number of activating sites or vacancies per unit length of dislocation, we have $Q_{max}^{-1} \propto N_0 l^2 \cong \eta_0/10$. It is plausible that η_0 will acquire a constant value at an early stage of deformation, determined by the balance between production and annihilation of vacancies. In this connection, it should be noted that the vacancy concentration in nickel is known to be independent of strain.[28]

In conclusion, it should be stated clearly that the crucial point upon which our mechanism must stand or fall is its prediction of the absence of Bordoni peaks in bcc pure metals. Although we believe that our results on zone refined iron lend substantial support to our point of view, the desirability of studying bcc metals of substantially lower total interstitial content (<0.0001 at. %) is evident.

VII. ACKNOWLEDGMENTS

The author wishes to express particular gratitude to Professor A. W. Lawson for his support and encouragement throughout the course of this work. He is also indebted to Professor M. H. Cohen, Professor C. S. Barrett, and Professor H. K. Birnbaum for many valuable discussions.

The design and firing of the explosive assembly pictured in Fig. 8 was carried out by Dr. G. R. Fowles and Dr. G. E. Duvall of the Standard Research Institute. Their expert cooperation made possible our study of shocked copper. Niobium specimens were kindly supplied by Dr. R. J. Wasilewski of E. I. du Pont de Nemours and Company. Zone refined iron was obtained through the courtesy of Dr. J. W. Halley, Dr. K. L. Fetters, and Dr. G. W. Rengstorff; it was purified by the latter under the project supported by the American Iron and Steel Institute.

The award of a fellowship by the Crane Company is also gratefully acknowledged.

[33] L. C. Weiner and M. Gensamer, Acta Met. 5, 692 (1957).
[34] T. S. Ke, Trans. Am. Inst. Mining, Met., Petrol., Engrs. 176, 448 (1948).

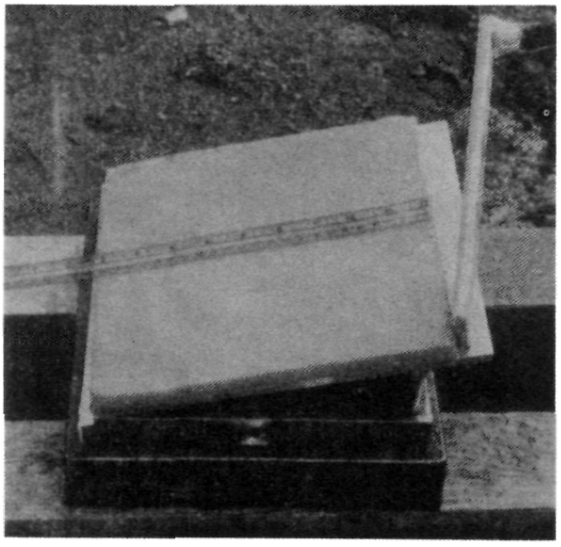

FIG. 8. Photograph of explosive shot assembly used in preparation of polycrystalline Cu specimen 5.